NACA RM L55E20c

NACA

RESEARCH MEMORANDUM

BEHAVIOR OF A CANTILEVER PLATE UNDER RAPID-HEATING CONDITIONS

By Louis F. Vosteen and Kenneth E. Fuller

Langley Aeronautical Laboratory
Langley Field, Va.

NATIONAL ADVISORY COMMITTEE
FOR AERONAUTICS

WASHINGTON

July 25, 1955

NATIONAL ADVISORY COMMITTEE FOR AERONAUTICS

RESEARCH MEMORANDUM

BEHAVIOR OF A CANTILEVER PLATE UNDER RAPID-HEATING CONDITIONS

By Louis F. Vosteen and Kenneth E. Fuller

SUMMARY

The temperature distributions encountered in thin solid wings subjected to aerodynamic heating induce thermal stresses that may effectively reduce the stiffness of the wing. The effects of this reduction in stiffness were investigated experimentally by rapidly heating the edges of a cantilever plate. The midplane thermal stresses imposed by the nonuniform temperature distribution caused the plate to buckle torsionally, increased the deformations of the plate under a constant applied torque, and reduced the frequency of the first two natural modes of vibration. By using small-deflection theory and employing energy methods, the effect of nonuniform heating on the plate stiffness was calculated. The theory predicts the general effects of the thermal stresses, but becomes inadequate as the temperature difference increases and plate deflections become large.

INTRODUCTION

One of the structural problems produced by nonuniform heating is a change in the effective stiffness of the structure caused by thermal stresses. This change in stiffness is not associated with a change in the material properties, but depends on the state of stress and may occur at stress levels well below those necessary to produce buckling. Laboratory demonstrations have shown that the natural frequency of a simplified wing structure can be effectively reduced by the nonuniform temperature distribution associated with rapid heating.

The type of temperature distribution produced by the aerodynamic heating of a thin missile wing is shown in figure 1. This figure (given in ref. 1) shows the variation in temperature across the chord of a solid double-wedge airfoil immediately following a 1g acceleration to Mach number 4 at 50,000 feet. The temperatures on the surface and at the midplane are shown. Such a temperature distribution produces

compressive stresses near the leading and trailing edges and tension in the central part of the wing. The effect of these stresses is a reduction in the stiffness of the structure that may be observed as an increased deformation under load or as a reduction in natural frequency. No quantitative data exist, however, which relate changes in frequency, and hence effective stiffness, to temperature distribution. The project to be discussed in this paper was devised to satisfy part of this need.

TEST PROCEDURE AND RESULTS

An arrangement was selected that required a simple test setup and that could be analyzed theoretically with relative ease. The test arrangement used is shown in figure 2. A nonuniform temperature distribution resembling that encountered by aerodynamically heated wings was produced by rapidly heating (with carbon-rod radiators) the longitudinal edges of a cantilever aluminum-alloy plate 1/4 inch thick and 20 inches square. The temperature distribution along the span of the plate was constant except for a slight decrease toward the tip. Figure 3 shows how the temperature on the edge and at the midchord varied during a test.

In figure 3 the temperature in degrees Fahrenheit of an edge and the midchord line is plotted against time in seconds. Heat is applied to the plate for about 16 seconds. During this time, the edge temperature rises almost linearly to 315° F at the peak of the heating cycle. When the heating stops, the temperature drops quickly and slowly levels off as the plate cools. The variation in temperature across the chord has been shown in figure 2 for a time in the heating cycle (10 seconds), at the time of maximum edge temperature (16.5 seconds), and during cooling (30 seconds). These distributions show that the temperature remains relatively low over the center half of the plate, but rises sharply near the heated edges.

Two investigations were made to determine the effect of the nonuniform temperature distribution on the stiffness. First, the deformations of the plate due to thermal stresses were obtained for various load conditions. Second, the changes in natural frequency of vibration during heating were investigated.

Deformations

Figure 4 shows the tip-rotation histories. The angle of rotation of the tip in degrees is plotted against time in seconds during heating and cooling for no external load and for applied torques of 400 inch-pounds in each direction. In each case, the plate deformed by rotating

torsionally about the midchord line. As the plate cooled, the deformations decreased and the plate returned to its original position. Note that the plate underwent an appreciable deformation without the application of an external load. This thermal buckling of the plate may be a significant factor in the control of missiles having solid fins. The plate rotated in the same direction regardless of whether heat was applied symmetrically or on either edge because of an initial twist. The increased deformations, which occurred when a constant torque was applied in the same direction as the initial twist, indicate an approximate superposition of the deformation induced by the thermal stresses on the initial static deflection. When a torque was applied in the opposite direction, the plate twisted in the direction of the applied torque, but the maximum twist was slightly less.

Natural Frequencies

It is difficult to detect the frequency changes of a plate under transient heating conditions because of the time required to establish resonance. For this reason the present investigation has so far been limited to the first bending and first torsion modes, inasmuch as a frequency history could be obtained for these two modes by striking the plate at regular intervals during the test.

Figure 5 shows how the frequencies of the first two modes varied during the test. Here, frequency of vibration in cycles per second has been plotted against time in seconds for the first bending and first torsion modes. The first bending frequency decreased from 19 cycles per second to 15 cycles per second at the point of maximum temperature gradient. This is a 21-percent reduction in frequency. The first torsion frequency begins at 48 cycles per second and drops to a minimum of 30 cycles per second - a reduction in natural frequency of about 35 percent. As the plate cools, both frequencies return to their original values. The small irregularity which occurs at the peak of the heating cycle has been observed in all the first-torsion-mode tests, but as yet its cause has not been determined.

THEORETICAL ANALYSIS AND COMPARISON WITH EXPERIMENTAL RESULTS

As a first approach to predicting the changes measured in these tests, small-deflection theory has been used. The analytical approach, which is a combination of the energy methods used to solve buckling and vibrational problems, is outlined in the appendix.

Deformations

A comparison of the predicted and actual effect of the temperature gradient on the torsional stiffness for the case of no vibration is shown in figure 6. Here the tip rotation in degrees has been plotted against the edge-to-center temperature difference ΔT in degrees Fahrenheit for an applied torque of 400 inch-pounds. Curves are shown for the period of heating (or increasing ΔT) and cooling (or decreasing ΔT). The small-deflection theory gives a reasonable approximation of the reduction in stiffness about halfway to the buckling temperature. Above this point, however, the small-deflection theory indicates that the plate deflections would increase more rapidly than actually occurs.

Natural Frequency

Figure 7 compares the results of the calculations with test results when there are no external loads and the plate is vibrating in the first torsion mode. In this figure the frequency in cycles per second has been plotted against temperature difference between the edge and the midchord line for the periods of increasing and decreasing ΔT. The small-deflection theory again approximates the frequency change about halfway to the critical buckling temperature. Above this value, the theory again overestimates the change. This disagreement occurs because the distortions have become large and the small-deflection theory is no longer valid. When the analysis is extended to include the effects of large deflections, more satisfactory agreement is expected at the critical ΔT.

Figure 8 shows a similar comparison of measured and calculated frequency as a function of time. The ratio of actual frequency to the initial uniform-temperature frequency is plotted against time in seconds. The calculated curve indicates that the theoretical critical-buckling temperature differential is reached in about 15 seconds. The small-deflection theory predicts that the plate would have lost all its stiffness at this point, but this is not the actual case. Since stiffness is proportional to the square of the frequency, the frequency decrease obtained indicates that only about half of the stiffness was lost as a result of the induced thermal stresses. As the plate cools and the temperature difference becomes less than half that required for buckling, the theory is again in fair agreement with the test results.

CONCLUDING REMARKS

Tests of a cantilever plate have shown that the midplane stresses imposed by a nonuniform temperature distribution can effectively reduce

the stiffness of the plate. This reduction in stiffness is reflected in the increased deformation under the action of a constant applied torque and also in the reduction of the natural frequency of vibration of the first two modes of the plate. By using small-deflection theory and by employing energy methods, the effect of nonuniform heating on the plate stiffness was calculated. The theory predicts the general effects of the thermal stresses, but is inadequate when the deformations become large. An extension of the analysis to account properly for large deflections is expected to give more satisfactory results near the critical temperature.

Langley Aeronautical Laboratory,
National Advisory Committee for Aeronautics,
Langley Field, Va., May 3, 1955.

APPENDIX

SMALL-DEFLECTION ANALYSIS OF CANTILEVER PLATE SUBJECTED TO NONUNIFORM TEMPERATURE DISTRIBUTION

By using small-deflection theory and by making several simplifying assumptions, an analysis of the effect of rapid heating on the deformations, natural frequencies of vibration, and torsional stiffness of a cantilever plate was made. The method used is outlined in this appendix.

Symbols

a	plate length, in.
A_{mn}, A_{ij}	arbitrary coefficients of deflection function
b	plate half-width, in.
D	plate flexural stiffness, $\frac{Et^3}{12(1 - \mu^2)}$
E	Young's modulus, psi
EI	bending stiffness, lb-in.^{2}
$(EI)_e$	effective bending stiffness, lb-in.^{2}
F	concentrated load, lb
F_{cr}	critical axial load, lb
g	gravitational constant, in./sec^2
GJ	torsional stiffness, lb-in.^{2}
$(GJ)_e$	effective torsional stiffness, lb-in.^{2}
K	arbitrary coefficient of stress function
p	distributed load, psi
t	plate thickness, in.

T	temperature, $^{\circ}F$
T_0	temperature of midchord, $^{\circ}F$
ΔT	difference in temperature between edge and midchord, $^{\circ}F$
ΔT_{cr}	critical temperature difference, $^{\circ}F$
U_B	potential energy of bending, in-lb
U_H	strain energy due to thermal expansion, in-lb
U_L	potential energy due to external load, in-lb
U_M	energy due to midplane stresses, in-lb
U_S	strain energy of midplane stresses, in-lb
$\omega^2 U_V$	kinetic energy of vibration, in-lb
w	deflection, in.
x	longitudinal coordinate measured from root, in.
y	transverse coordinate measured from midchord line, in.
α	coefficient of thermal expansion, $\frac{\text{in.}}{\text{in.}-^{\circ}F}$
ζ	arbitrary exponent in temperature distribution
θ	tip rotation, deg
θ_o	tip rotation when $\Delta T = 0$, deg
μ	Poisson's ratio
γ	specific weight, lb/cu in.
σ_x	longitudinal direct stress, psi
σ_y	transverse direct stress, psi
τ_{xy}	shear stress, psi

ϕ stress function

ω frequency, cps

ω_o frequency when $\Delta T = 0$, cps

Temperature Distribution

The temperature is assumed to be constant through the thickness of the plate and along the span; the distribution across the chord is represented by the simple power law

$$T = T_o + \Delta T\left(\frac{y}{b}\right)^{\zeta} \tag{1}$$

which involves the edge-to-midchord temperature difference ΔT and the power ζ required to describe the measured chordwise temperature distribution. The power ζ, which varies during a test, determines how sharply the temperature rises near the edges of the plate. In order to find how ζ varied, a curve of the form given in equation (1) was fitted to the chordwise temperature distributions measured at various times during a test. At the start of heating ζ is very large, but it decreases to about 4 at the peak edge temperature, continues to drop as the plate cools, and reaches a value of about 2 at the end of the test (about 35 seconds after the peak temperature). The temperature distribution given by equation (1) fits the measured distribution rather well during heating but becomes increasingly poor as the plate cools.

Thermal Stresses

The plate is assumed to be in a state of plane stress and all stresses are assumed to be in the elastic range of the material. The assumption also has been made that the material properties of the plate do not change with temperature. Thermal stresses are given by the relationships

$$\left.\begin{aligned} \sigma_x &= \frac{\partial^2 \phi}{\partial y^2} \\ \sigma_y &= \frac{\partial^2 \phi}{\partial x^2} \\ \tau_{xy} &= -\frac{\partial^2 \phi}{\partial x\, \partial y} \end{aligned}\right\} \tag{2}$$

where ϕ is the Airy stress function (see ref. 2) assumed to be given by

$$\phi = KE\alpha\,\Delta T\left(x^2 - a^2\right)^2\left(y^2 - b^2\right)^2 \tag{3}$$

This function satisfies the boundary condition that the stresses (eqs. 2) all vanish on the free boundaries ($x = a$ and $y = \pm b$).

In order to evaluate the arbitrary constant in the stress function (eq. 3), the method of minimum complementary energy is used. The expression can be written simply as

$$\frac{\partial}{\partial K}\left(U_S + U_H\right) = 0 \tag{4a}$$

where

$$\left.\begin{aligned} U_S &= \frac{1}{2E}\int_0^a \int_{-b}^{b}\left[\sigma_x^2 + \sigma_y^2 - 2\mu\sigma_x\sigma_y + 2(1+\mu)\tau_{xy}^2\right]dx\,dy \\ U_H &= \int_0^a \int_{-b}^{b} \alpha T\left(\sigma_x + \sigma_y\right)dx\,dy \end{aligned}\right\} \tag{4b}$$

The first integral is the usual strain-energy expression and the second represents the strain energy due to thermal expansion of the plate. (See ref. 3.) By using equation (1) for the temperature T and equations (2) and (3) for the stresses, the constant K may be evaluated from equation (4a). When $\frac{a}{b} = 2$ the result is

$$K = \frac{-2.722}{a^6}\,\frac{\zeta}{(\zeta + 3)(\zeta + 1)} \tag{5}$$

Effect of Temperature Gradient on Deflections and Natural Frequencies

To find the effect of temperature gradient on the deflections and natural frequencies, another minimum-energy method is used. Deflections are represented by the power series

$$w = \sum_{m=1}^{\infty}\sum_{n=1}^{\infty} A_{mn}x^{m+1}y^{n-1} \tag{6}$$

which satisfies the boundary conditions (the slope and deflection are zero at the root, $x = 0$). The undetermined coefficients of the deflection function may be evaluated by minimizing the change in energy during deflection with respect to each of these coefficients. The expression can be written as

$$\frac{\partial}{\partial A_{ij}}\left(U_B + U_M - \omega^2 U_V + U_L\right) = 0 \tag{7a}$$

where

$$\left.\begin{aligned} U_B &= \frac{D}{2}\int_0^a \int_{-b}^{b} \left[\left(\frac{\partial^2 w}{\partial x^2}\right)^2 + \left(\frac{\partial^2 w}{\partial y^2}\right)^2 + 2\mu \frac{\partial^2 w}{\partial x^2}\frac{\partial^2 w}{\partial y^2} + 2(1-\mu)\left(\frac{\partial^2 w}{\partial x \partial y}\right)^2\right] dx\, dy \\ U_M &= \frac{t}{2}\int_0^a \int_{-b}^{b} \left[\sigma_x\left(\frac{\partial w}{\partial x}\right)^2 + \sigma_y\left(\frac{\partial w}{\partial y}\right)^2 + 2\tau_{xy}\frac{\partial w}{\partial x}\frac{\partial w}{\partial y}\right] dx\, dy \\ U_V &= \frac{2\pi^2 \gamma t}{g}\int_0^a \int_{-b}^{b} w^2 dx\, dy \\ U_L &= \int_0^a \int_{-b}^{b} pw\, dx\, dy \end{aligned}\right\} \tag{7b}$$

The first integral is the energy due to bending, the second is the energy imposed by midplane thermal stresses (obtained from eqs. 2 and 3), the third is the kinetic energy of vibration, and the fourth is the potential energy resulting from any external loads applied perpendicular to the plane of the plate. (See refs. 4 and 5.)

Analysis of torsional deflections.- The thermal buckling which occurred when the longitudinal edges of the cantilever plate were heated resulted in torsional deformations which were similar to the deformations that took place when a constant torque was applied to the plate tip. Of the first two modes of vibration, both of which experienced a reduction in natural frequency, the first torsion mode underwent the largest change. Therefore, the remainder of the analysis has been restricted to torsional deformations. Six terms of the deflection function which are antisymmetrical in y have been used. The deflection is then given as

$$\begin{aligned} w = {} & A_{12}x^2y + A_{14}x^2y^3 + \\ & A_{22}x^3y + A_{24}x^3y^3 + \\ & A_{32}x^4y + A_{34}x^4y^3 \end{aligned} \tag{8}$$

When there is no external load or vibration, the solution of equation (7a) gives the temperature difference necessary to produce thermal buckling. For a square plate $\left(\frac{a}{b} = 2\right)$ this difference is

$$\Delta T_{cr} = \frac{-49.98D}{a^8 tKE\alpha} \tag{9}$$

When the value of K given by equation (5) is used, equation (9) becomes

$$\Delta T_{cr} = \frac{18.36D}{a^2 tE\alpha} \frac{(\zeta + 3)(\zeta + 1)}{\zeta} \tag{10}$$

Since the flexural stiffness D also contains the modulus E, the critical temperature difference depends only on the plate geometry, the coefficient of thermal expansion, and Poisson's ratio.

For the case of no external load or heating, the frequency of the first torsion mode of a square plate $\left(\frac{a}{b} = 2\right)$ is found to be

$$\omega_o = \frac{4.185}{a^2\pi}\sqrt{\frac{Dg}{\gamma t}} \tag{11}$$

The frequency given by this relationship is slightly higher than that obtained in the experiments. This is due largely to insufficient clamping of the plate root. For the purpose of comparing measured and calculated results, the theoretical plate was assumed to be slightly longer than the actual plate so that the measured and calculated frequencies would be the same at the start of the test.

If no heat is applied and the plate is not vibrating, the angle of twist of the tip (assuming that the tip remains a straight line) resulting from a couple of magnitude 2Fb produced by applying a concentrated load F at the tips (a, $\pm$b) of a square plate $\left(\frac{a}{b} = 2\right)$ is

$$\theta_o = 32.18 \frac{2Fb}{D} \tag{12}$$

Approximate interaction equations.- The deflection modes of the plate for first-torsion-mode vibration, thermal buckling, and applied torques at the tip are all very similar. If these three modes are assumed to be identical, the deflection can then be expressed as a function with only one arbitrary coefficient, and simple interaction

equations can be obtained. For heating with no external load, the ratio of actual frequency to the initial uniform-temperature frequency is found to be

$$\frac{\omega}{\omega_o} = \sqrt{1 - \frac{\Delta T}{\Delta T_{cr}}} \tag{13}$$

For heating with no vibration, the ratio of the angle of twist of the tip to the angle at uniform plate temperature for a constant torque is

$$\frac{\theta}{\theta_o} = \frac{1}{1 - \frac{\Delta T}{\Delta T_{cr}}} \tag{14}$$

The frequency of vibration is proportional to the square root of the torsional stiffness GJ, and the angle of twist is inversely proportional to the stiffness. Hence, in this simple case it is apparent from equations (13) and (14) that

$$\frac{(GJ)_e}{GJ} = 1 - \frac{\Delta T}{\Delta T_{cr}} \tag{15}$$

where GJ is the torsional stiffness of the unstressed plate and $(GJ)_e$ is the effective stiffness of the plate when subjected to thermal stresses.

It is of interest to note that a relationship similar to equation (15) exists for a simple beam subjected to an axial load. The ratio of the effective flexural stiffness of the loaded beam to that of the unloaded beam is

$$\frac{(EI)_e}{EI} = 1 - \frac{F}{F_{cr}} \tag{16}$$

where F is the axial load (positive for tension, negative for compression) and F_{cr} is the load necessary to produce column buckling.

The simple expressions given in equations (13) and (14) very closely approximate the results obtained by solving equation (7a) for related values of frequency, temperature, and twist.

REFERENCES

1. Kaye, Joseph: The Transient Temperature Distribution in a Wing Flying at Supersonic Speeds. Jour. Aero. Sci., vol. 17, no. 12, Dec. 1950, pp. 787-807, 816.

2. Timoshenko, S., and Goodier, J. N.: Theory of Elasticity. Second Ed., McGraw-Hill Book Co., Inc., 1951, p. 169.

3. Heldenfels, Richard R., and Roberts, William M.: Experimental and Theoretical Determination of Thermal Stresses in a Flat Plate. NACA TN 2769, 1952.

4. Timoshenko, S.: Theory of Elastic Stability. McGraw-Hill Book Co., Inc., 1936, pp. 305-323.

5. Timoshenko, S.: Vibration Problems in Engineering. Second Ed., D. Van Nostrand Co., Inc., 1937, p. 423.

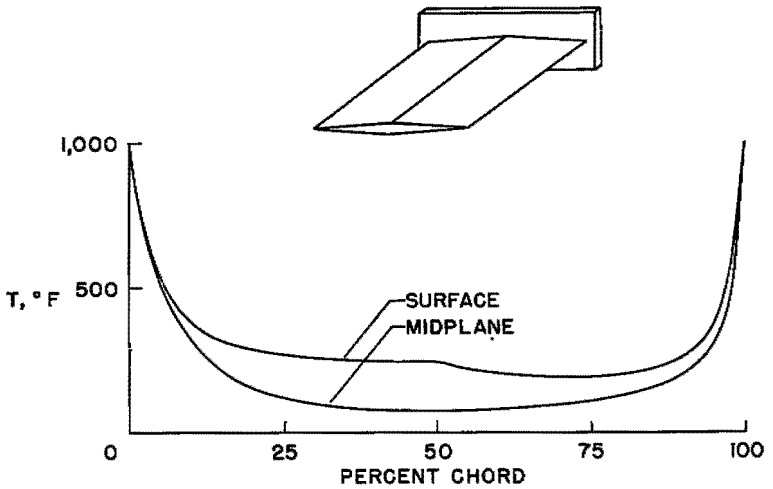

Figure 1.- Chordwise temperature distributions in an aerodynamically heated airfoil (ref. 1, fig. 11).

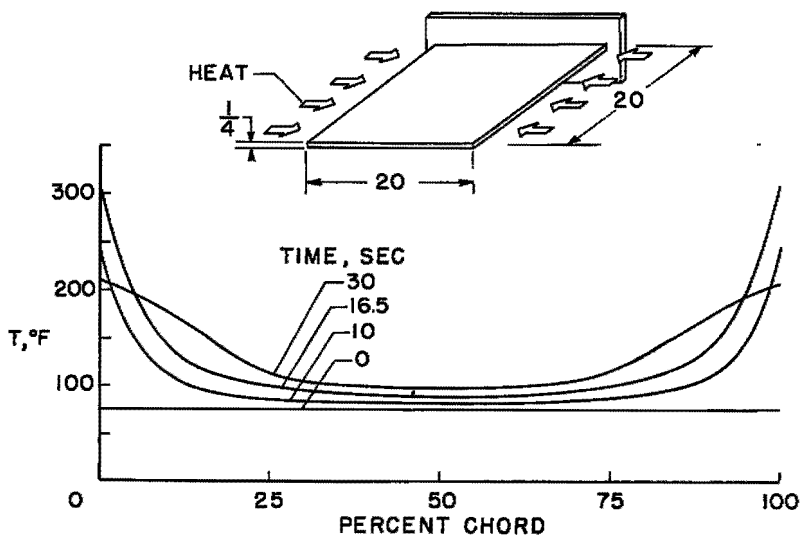

Figure 2.- Measured chordwise temperature distributions of a radiantly heated cantilever plate.

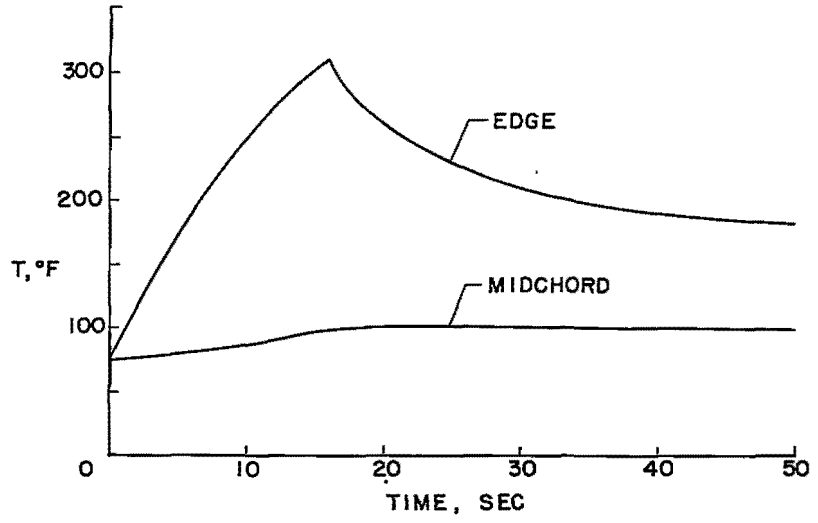

Figure 3.- Measured temperature histories for an edge and the midchord line.

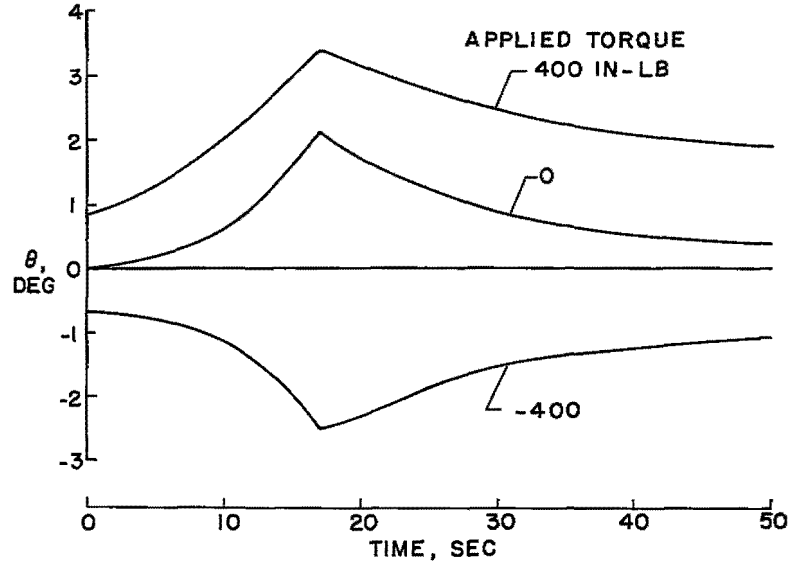

Figure 4.- Measured tip-rotation histories for applied tip torques of 0 and ±400 in-lb.

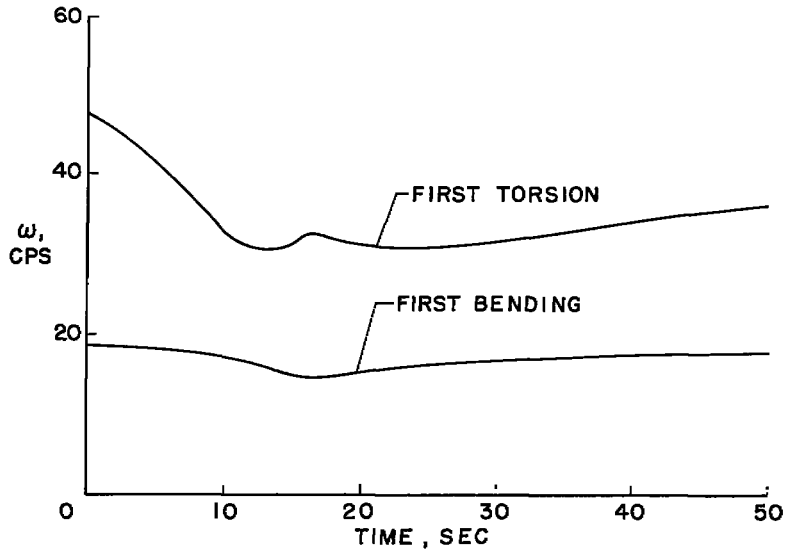

Figure 5.- Measured frequency histories for the first bending and first torsion modes.

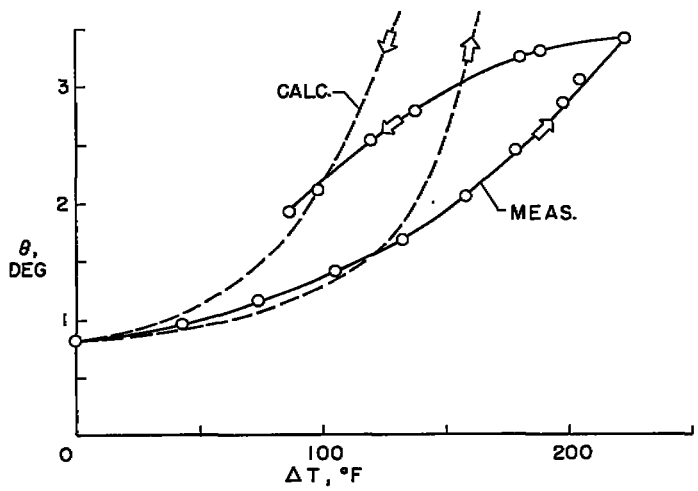

Figure 6.- Comparison of measured and calculated tip rotations for an applied tip torque of 400 in-lb.

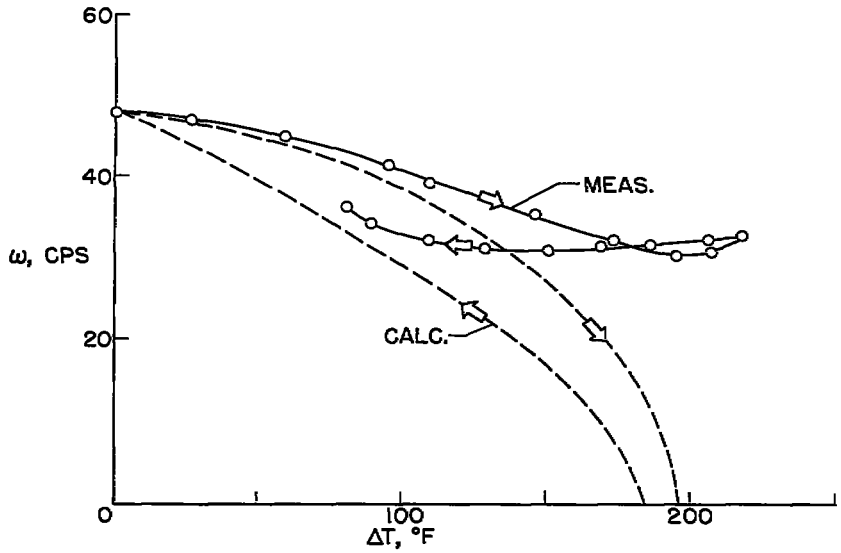

Figure 7.- Comparison of measured and calculated frequency changes for the first torsion mode.

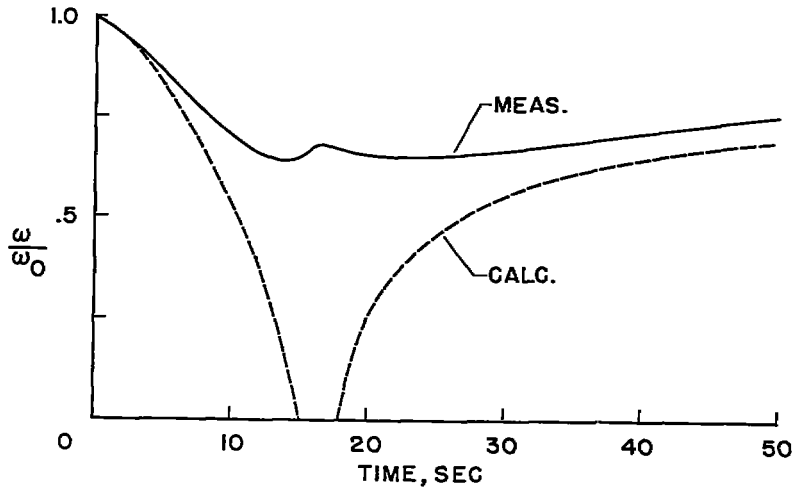

Figure 8.- Comparison of measured and calculated frequency histories for the first torsion mode.